# Identification of roll damping coefficient using the free rotation method

Ionut BUNESCU*,[1,2], Mihai-Victor PRICOP[1], Mihaita-Gilbert STOICAN[1], Mihai-Vladut HOTHAZIE[1,2]

*Corresponding author
*,[1]INCAS – National Institute for Aerospace Research “Elie Carafoli”,
B-dul Iuliu Maniu 220, Bucharest 061136, Romania,
bunescu.ionut@incas.ro
[2]Doctoral School of Aerospace Engineering,
POLITEHNICA Bucharest National University for Science and Technology,
Splaiul Independentei 313, 060042, Bucharest, Romania

DOI: 10.13111/2066-8201.2024.16.1.2

*Received: 05 January 2024/ Accepted: 14 February 2024/ Published: March 2024*
Copyright © 2024. Published by INCAS. This is an “open access” article under the CC BY-NC-ND license (http://creativecommons.org/licenses/by-nc-nd/4.0/)

***Abstract:*** *The free rotation method represents the simplest method for roll damping coefficient identification in experimental aerodynamics. To apply this method, it is necessary to spin the model to a desired angular velocity and then release the model to spin freely under flow conditions, recording the variation in time of the model’s rolling rate. Thus, applying the logarithmic decrement formula at any roll rate between near zero and the desired angular velocity, the roll damping moment will be calculated. This paper presents the application of the free rotation method on raw data obtained for different Mach numbers and incidences, considering different regression functions, time windows and their implications. Last but not least, the necessary correction methods and their impact on the results are presented.*

***Key Words:*** *Roll damping coefficient, experimental aerodynamics, free rotation method, regression methods, wind tunnel*

## 1. INTRODUCTION

This paper extends the work initiated in [1] focusing on the free rotation method. Reference [1] presents the free rotation method and provides/ gives slightly different results than the forced rotation method, considering that there is no regression function for roll rate variation over time. Herein, to improve the accuracy of the results obtained by the free rotation method, several regression functions are considered for fitting and smoothing the data, so that the roll rate variation in time is described by a uniform function instead of a noisy time series. Furthermore, this paper presents the influences of the regression function on the roll damping coefficient and explains why the exponential damping function, assumed to be the natural choice, is not the best fit to the data.

To validate the procedure for data processing, two comparisons with reference data are performed: the roll damping coefficient ($C_{lp}$) variation with Mach number at 0° AoA, and the roll damping coefficient variation with angle of attack at Mach 2.5. The reference data include ballistic tests [2] and wind tunnel tests performed by the free rotation method [3] and the forced rotation method [4], [8]. The analyzed cases include four Mach numbers representative for subsonic, transonic and supersonic regimes (0.4, 0. 95, 1.6 and 2.5) at 0° AoA and four incidences (0°, 5°, 12.5° and 20°) at Mach 2.5. These cases were chosen given the available reference data in relation to the capacities of the installation.

The wind tunnel facility where the tests were carried out is the Trisonic Wind Tunnel (TWT) of The National Institute for Aerospace Research "Elie Carafoli" (INCAS) described in [5]. A roll damping rig described in [1] is mounted on the port-sting adapter of the facility in order to evaluate the roll damping coefficient. This rig is developed to be independent of the facility control system and comprises a DC motor that spins the model, an electromagnetic clutch between the motor and the model axis and a Hall-effect sensor that measures the roll rate of the model.

## 2. METHODOLOGY DESCRIPTION

The experimental campaign was performed using the free rotation method which consists in recording the roll rate time history while the angular velocity of the model is damping after an initial spinning at a desired rate. Then the variation of the roll rate in time is used to calculate the roll damping moment with the following equation, as in [6]:

$$M_{xp} = I_x \frac{\ln \frac{p_2}{p_1}}{t_2 - t_1}, \tag{1}$$

where $p_1$ and $p_2$ are the angular velocities at $t_1$ and $t_2$ times, and $I_x$ is the moment of inertia around the x axis.

As shown in [6] and [1], the roll damping moment is tare corrected, subtracting the contribution of bearings friction from the entire roll damping moment, to retain the clean aerodynamic contribution of the roll damping coefficient $M_{xpa}$. Thus, with corrected roll damping moment, the roll damping coefficient is given by the following equation:

$$C_{lp} = \frac{\partial C_l}{\partial \frac{pd}{2V_\infty}} = M_{xpa} \frac{2 \cdot V_\infty}{q_\infty \cdot A \cdot d^2}, \tag{2}$$

Further on, according to [1], the roll damping coefficient has to be corrected with the geometry deviation by averaging the results obtained for clockwise and counter clockwise rotation.

The wind tunnel model used to perform the experimental campaign is a common research model for dynamic tests, adopted by STAI (Supersonic Tunnels Association International) and AGARD (The Advisory Group for Aerospace Research and Development), as in [4].

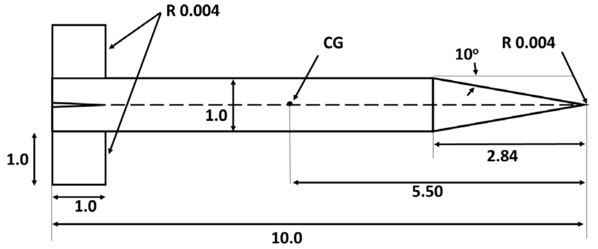


Figure 1 – BFM lateral view

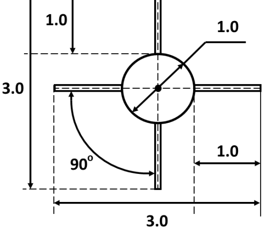


Figure 2 – BFM front view

This model is named Basic Finner Model, but is also known as Army Navy Finner and consists in a cone-cylinder body with four square and sharp fins as shown in Figure 1 and Figure 2.

The considered model has been scaled to a diameter of 60 mm and a moment of inertia equal to 7.3 g·m$^2$. The reference dimensions are the model diameter and its cross section area.

To evaluate the model manufacturing accuracy, an optical scan of all components was performed.

This scanning shows that the model surface presents deviations from the ideal geometry generated in the manufacturing process. Figure 3 presents the geometry deviation of the BFM body and fins.

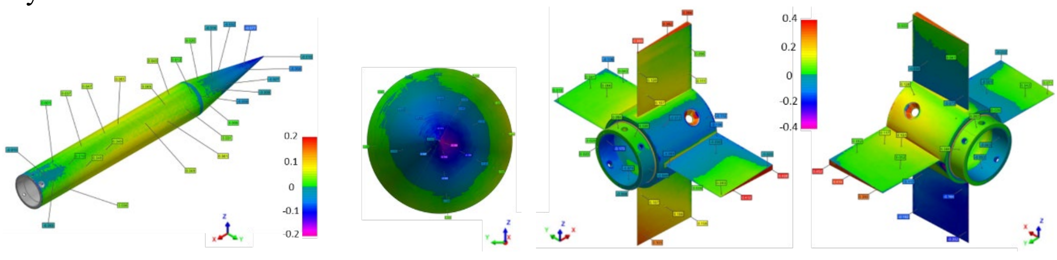


Figure 3 – Geometry deviation on BFM body and fins

The deviations range is between -0.4 mm and 0.4 mm which has the potential to generate additional aerodynamic momentum under flow condition due to the geometry. Thus, a correction method [1] for geometry deviation is required to obtain accurate results.

## 3. REGRESSION METHODS

To determine the values of roll damping coefficient, several nonlinear regression functions are considered. These functions are presented in equations (3) - (8) below.

The LHS term, $y_i(x)$, represents the dependent variable of the regression function considered, the $a_i$ and $b_i$ represent the decision variables, and $x$ represents the independent variable, which in this case is time [7].

Second-order polynomial function:

$$y_{p2}(x) = a_1 \cdot x^2 + a_2 \cdot x + a_3 \tag{3}$$

Two terms Gauss function:

$$y_{g2}(x) = a_1 \cdot e^{-\left(\frac{x-b_1}{c_1}\right)^2} + a_2 \cdot e^{-\left(\frac{x-b_2}{c_2}\right)^2} \tag{4}$$

Two terms sinusoidal function:

$$y_{s2}(x) = a_1 \cdot \sin(b_1 \cdot x + c_1) + a_2 \cdot \sin(b_2 \cdot x + c_2) \tag{5}$$

Second-order Fourier function:

$$y_{f2}(x) = a_0 + a_1 \cdot \cos(x \cdot p) + b_1 \cdot \cos(x \cdot p) + a_2 \cdot \cos(2 \cdot x \cdot p) + b_2 \cdot \cos(2 \cdot x \cdot p) \tag{6}$$

where $p = \frac{2\pi}{\max(x) - \min(x)}$

Two terms exponential function:

$$y_{e2}(x) = a_1 \cdot e^{b_1 \cdot x} + a_2 \cdot e^{b_2 \cdot x} \tag{7}$$

One term exponential function:

$$y_{e1}(x) = ae^{bx} \tag{8}$$

The last regression function, equation (8), represents the formula of roll rate variation in time when a model is damping, as presented in [6].

This equation is applicable when the damping process is generated only by the aerodynamic moment. In reality, the bearings friction and geometry deviations make this equation not applicable. However, this function is considered to quantify the differences between the perfect scenario, where extra loads are missing, and the real scenario, where extra loads do exist.

The decision variables of each regression function are obtaining by the least square method which consists in an optimization process where the objective function is the sum of the squared differences between the observed value and the fitted value predicted by the regression function [7] as shown below:

$$\min_{\{a_i, b_i\}} J = \sum_{i=1}^{N} [\tilde{y}_i - y(x_i)]^2 \tag{9}$$

Because nonlinear functions present many decision variables, the optimization process is solved numerically using a gradient-based algorithm. Thus, for each dataset, the decision variables and root mean square error (RMSE) are computed in order to compare the accuracy of each function. A more suitable fitting objective function than (9) is the modified version (10), which produces better results.

$$RMSE = \sqrt{\sum_{i=1}^{N} \frac{[\tilde{y}_i - y(x_i)]^2}{N}} \tag{10}$$

The RMSE value is used to establish which regression function is more suitable to fit the variation of angular speed in time in order to determine the roll damping coefficient considering the free rotation method.

Moreover, this value considers the effect of oscillatory shape of the roll damping coefficient versus roll angle, which is amplified at high angles of attack, when the flow is asymmetric with respect to the model.

## 4. RESULTS AND DISCUSSIONS

### 4.1 Test cases

This study considers several test cases in order to obtain the dependency of the roll damping coefficient with Mach number and with angle of attack. The first test case considers 0° AoA and four different Mach numbers, while the second test case considers Mach=2.5 and four different angles of attack.

For Mach variation of the roll damping coefficient, four different Mach numbers were considered representative for subsonic regime (Mach=0.4), transonic regime (Mach=0.95), low-supersonic regime (Mach=1.6) and high-supersonic regime (Mach=2.5).

The variations of roll rate versus time starting from 1000 rpm for each Mach case are presented in the figures below:

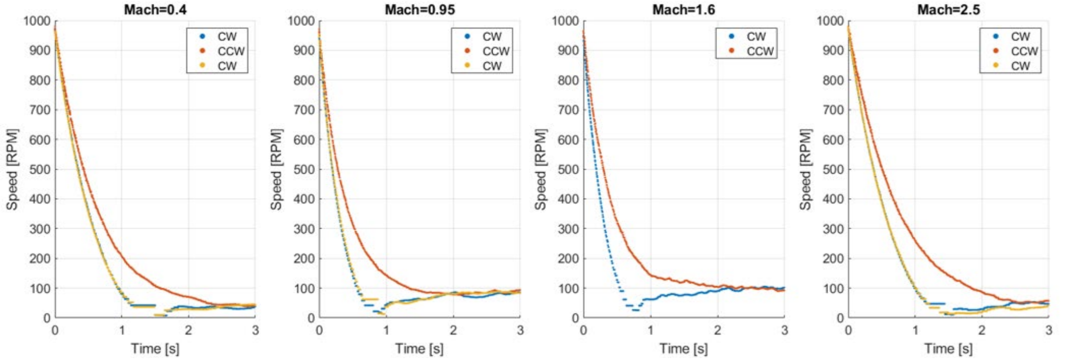


Figure 4 – 0° AoA analyzed cases at various Mach numbers

Each Mach case presents at least two data sets which are obtained spinning the model clockwise (CW) and counterclockwise (CCW).

It can be observed that depending on the direction of spinning, damping is faster in CW case or slower in CCW case.

Also, where the third data set is available, it can be observed that the variation trend aligns very well with the first data set.

Regarding the angle of attack dependency of the roll damping coefficient, four different incidences of the model are considered: 0°, 5°, 12.5° and 20°.

The figures below show the time damping of the spinning rate starting with 1000 rpm. Experiments were performed for AoA values of 0° and 20° in both CW and CCW spin direction, while the AoA values of 5° and 12.5° were performed only in the CW spin direction.

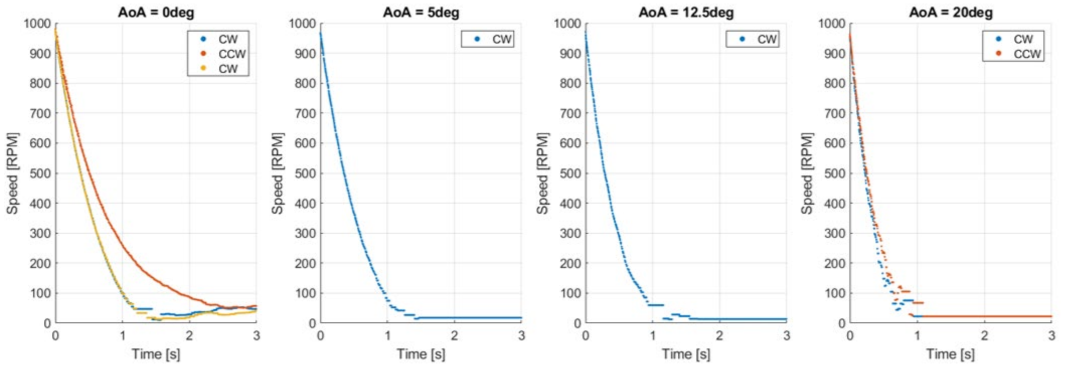


Figure 5 – Mach 2.5 analyzed cases at various angle of attack

In case of AoA=0°, the CW and CCW results have different variation trends, while in case of AoA=20°, the CW and CCW results have similar variation trends with small differences.

At small AoA values as 0° and 5°, the variation trends of roll rate are smooth, while at higher AoA values as 12° and 20°, the variation trend is oscillatory.

The effect of geometry deviation creates a parasitic roll moment, spinning in CCW direction, with the obvious effect that the roll rate damping is higher for the CW and smaller for the CCW.

### 4.2 Data fitting

The data acquisition system often produces scattered results due to electromagnetic noise, mechanical imperfections and acquisition sampling rate. Processing these results to determine the roll damping coefficient implies considerable errors, thus the recommended method to avoid erroneous results is to find the function that approximates with the best accuracy the raw data set, such that the roll damping coefficient is determined on a smoothed curve.

The considered regression functions for raw data fitting are applied for each test case. Below are presented two cases of data fitting application, showing the variation of angular velocity with time and the variation of roll damping coefficient with angular velocity for Mach=2.5, AoA=0° and 20°.

Figure 6 presents the speed damping in time for Mach 2.5, AoA=0° test case, while Figure 7 presents the roll damping coefficient variation with angular speed.

Both figures include six curves that correspond to the regression functions applied, the last one (*exp1*) representing the ideal damping variation, that is an exponential decay of the roll rate in time and a constant roll damping coefficient with roll.

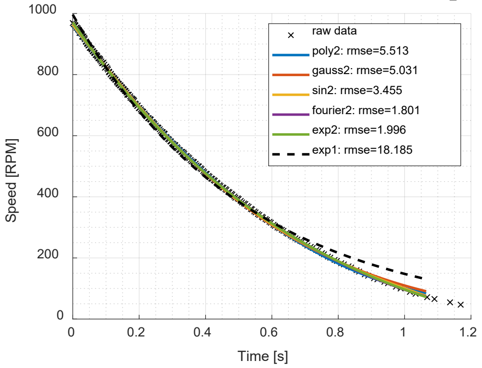


Figure 6 – Time variation of angular velocity at Mach 2.5, AoA = 0°

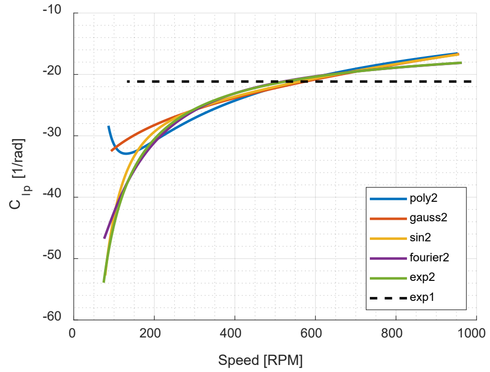


Figure 7 – Roll damping coefficient variation with angular velocity at Mach 2.5, AoA = 0°

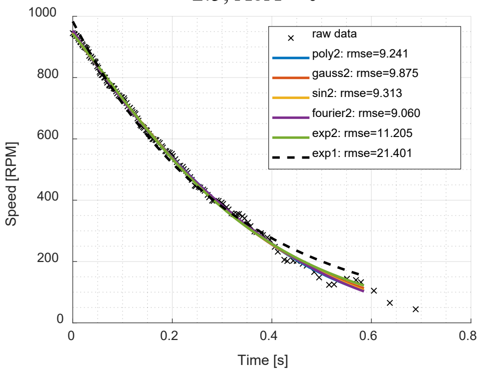


Figure 8 – Time variation of angular velocity at Mach 2.5, AoA = 20°

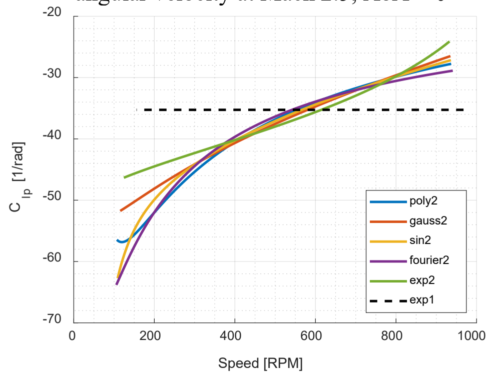


Figure 9 – Roll damping coefficient variation with angular velocity at Mach 2.5, AoA = 20°

Figure 8 and Figure 9 present similar variations to those in Figure 6 and Figure 7 but for Mach 2.5 and AoA=20°. In this case, the raw data present oscillations due to the variation of the roll momentum with roll angle which implies larger root mean square errors. It can be seen that the first five fitted curves fit the raw data set almost perfectly presenting small root mean square errors, while the sixth fitted curve which has to describe the damping phenomenon presents significant deviations especially at smaller angular velocities. The smallest errors are obtained for the second order Fourier function (6) while the other regression functions presents higher errors. However, the one-term exponential function presents the largest errors for both cases. Figure 7 and Figure 9 show that the roll damping coefficient variation trends have an asymptotic behavior with roll rate increasing. This phenomenon is due to the aerodynamic tare which becomes significant at small roll rates and negligible at higher roll rates. The aerodynamic tare represents the friction moments from bearings due to the aerodynamic loads, which is very difficult to subtract from the total roll damping coefficient. The mechanical tare due to the model weight was evaluated by spinning the model in vacuum chamber conditions and then subtracting it from the total roll damping coefficient. The asymptotic behavior of the roll damping variation trends is more pronounced in the AoA=0°, Figure 7, where the normal force is zero and the bearings are loaded only with axial force. In the AoA=20° case, Figure 9, where the bearings are loaded with both normal and axial force, the variation trend did not present a strong converging behavior.

The data fittings described above for all test cases produce the roll damping coefficient for the clockwise spin direction and for the counterclockwise spin direction. Table 1 presents the roll damping coefficients obtained for different Mach numbers at AoA=0°.

Table 1 – Roll damping coefficient obtained with different regression functions for different Mach regimes at 0° angle of attack

| | Mach 0.4 | | Mach 0.95 | | Mach 1.6 | | Mach 2.5 | |
|---|---|---|---|---|---|---|---|---|
| Method | CW | CCW | CW | CCW | CW | CCW | CW | CCW |
| Polynomial 2 | -17.77 | -12.64 | -17.57 | -9.31 | -22.51 | -21.20 | -18.23 | -12.56 |
| Gauss 2 | -19.71 | -17.09 | -20.60 | -17.30 | -27.18 | -23.23 | -18.34 | -15.33 |
| Sinus 2 | -18.39 | -14.62 | -18.50 | -12.09 | -23.46 | -21.43 | -18.40 | -14.27 |
| Fourier 2 | -20.03 | -16.65 | -20.71 | -15.47 | -26.05 | -25.08 | -19.91 | -15.48 |
| Exponential 2 | -19.89 | -17.35 | -23.07 | -16.82 | -31.26 | -29.11 | -19.90 | -16.24 |
| Exponential 1 | -19.16 | -15.67 | -20.09 | -14.20 | -26.09 | -24.01 | -18.96 | -14.78 |

Table 2 presents the roll damping coefficients obtained for different incidences at Mach=2.5. Both AoA values of 5° and 12.5° test cases present only clockwise spin direction results, while results are available for AoA values of 0° and 20° for both spin directions.

Table 2 – Roll damping coefficient obtained with different regression functions for different incidences at Mach number 2.5

| | AoA=0° | | AoA=5° | | AoA=12.5° | | AoA=20° | |
|---|---|---|---|---|---|---|---|---|
| Method | CW | CCW | CW | CCW | CW | CCW | CW | CCW |
| Polynomial 2 | -18.23 | -12.56 | -19.28 | - | -23.80 | - | -30.53 | -27.21 |
| Gauss 2 | -18.34 | -15.33 | -19.66 | - | -24.56 | - | -29.14 | -26.82 |
| Sinus 2 | -18.40 | -14.27 | -20.10 | - | -24.24 | - | -29.88 | -27.61 |
| Fourier 2 | -19.91 | -15.48 | -21.23 | - | -25.82 | - | -31.76 | -28.81 |
| Exponential 2 | -19.90 | -16.24 | -21.23 | - | -23.41 | - | -26.51 | -31.10 |
| Exponential 1 | -18.96 | -14.78 | -20.30 | - | -24.37 | - | -29.56 | -28.31 |

It is observed that the one-term exponential function produces higher values for the roll damping coefficient. The values obtained using this function are used only as a reference for the other regression functions. Moreover, the results obtained for clockwise and counterclockwise spin direction present significant differences as shown in Figure 4 and Figure 5. These differences are explained by the geometry deviation effect which creates a parasitic roll moment that alternates the roll damping coefficient. As shown in [1], to correct the roll damping coefficient with geometry deviations effect it is sufficient to average the results obtained for CW and CCW spin direction.

### 4.3 Comparison with reference data

In order to compare the obtained results with reference data, Table 3 presents the values of the roll damping coefficient as an average of considered regression functions results.

Table 3 – Averaged roll damping coefficient for AoA=0° and Mach 2.5

| | AoA = 0° | | | | Mach = 2.5 | | | |
|---|---|---|---|---|---|---|---|---|
| | Mach=0.4 | Mach=0.95 | Mach=1.6 | Mach=2.5 | AoA=0° | AoA=5° | AoA=12.5° | AoA=20° |
| CW | -19.16 | -20.09 | -26.09 | -18.96 | -18.96 | -20.30 | -24.37 | -29.56 |
| CCW | -15.67 | -14.20 | -24.01 | -14.78 | -14.78 | - | - | -28.31 |
| Average | -17.41 | -17.14 | -25.05 | -16.87 | -16.87 | -20.30 | -24.37 | -28.94 |

These results are compared with reference data from NOL (Naval Ordnance Laboratory) according to [3], BRL (Ballistic Research Laboratory) according to [2] and NAL (National Aeronautical Laboratory) according to [4].

Figure 10 presents the variation of the roll damping coefficient ($C_{lp}$) with the Mach number at 0° angle of attack. This figure shows three reference data sets (NOL, BRL and NAL) and three obtained data sets (CW spin, CCW spin and averaged).

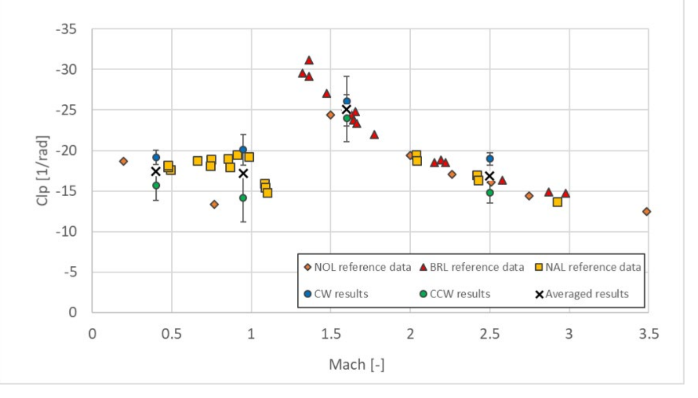


Figure 10 – Roll damping coefficient variation with Mach number at AoA=0°

The CW data set tends to overpredict the reference data, while the CCW data set tends to underpredict the reference data. The average of CW and CCW spin direction fits perfectly with reference data sets at any Mach number. It can be stated that the obtained results are in good agreement with the reference data. Figure 11 presents the variation of the roll damping coefficient ($C_{lp}$) with the angle of attack at 2.5 Mach number. This figure shows only one reference data set available in NAVORD report [3] and two obtained data sets for CW and CCW spin direction.

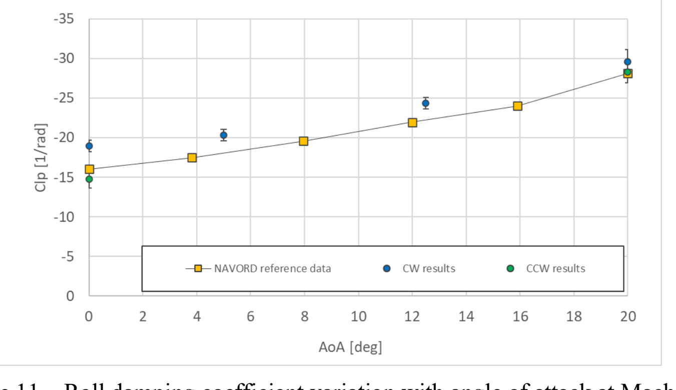


Figure 11 – Roll damping coefficient variation with angle of attack at Mach 2.5

It is observed that also in this case, the CW results tend to overestimate the roll damping coefficient while the CCW results tend to be slightly under the reference data. However, the average between the CW and CCW results present good accuracy with respect to reference data.

It is important to mention that, for both studies, the confidence intervals are small and offer acceptable results.

Also, it is very important to apply the geometry deviation correction averaging the CW and CCW results.

To avoid this correction, it is recommended to spin the model at higher velocities so that the parasitic moment due to geometry deviation becomes insignificant.

## 5. CONCLUSIONS

In conclusion, six regression functions have been presented as solutions for data fitting of the roll rate decay in time to evaluate the roll damping coefficient using the free rotation method. It can be concluded that the function which describe the damping (exponential function) did not work due to other elements such as aerodynamic tare and geometry deviation effects. Moreover, the first five functions considered showed good results relative to reference data, although there are small differences.

This study highlighted the sensitivity of the data processing explaining how different regression functions give different results. Moreover, the correction methods are necessary to obtain accurate results which did not include bearings friction moments or aerodynamic moment generated by geometry deviations.

The results obtained with different regression functions have been presented in comparison with the reference data for two cases: Mach variation at AoA=0° and incidence variation at Mach 2.5. Both comparisons showed that the spin direction influences the roll damping coefficient. The CW spin direction tends to overestimate the roll damping coefficient while the CCW spin direction tends to underestimate the roll damping coefficient. The simplest method to correct this effect of geometry deviation is to average the results obtained with both CW and CCW spin direction. Also, to avoid the necessity of correction due to geometry deviation, it is recommended to spin the model at higher angular velocities. In this way the effect of geometry deviation and aerodynamic tare becomes insignificant with respect to roll damping moment.

## ACKNOLEDGEMENT

This work was fully supported by the contract 671PED/ 21.06.2022 (PN-III-P2-2.1-PED-2021-2215), with the title “High Speed Aerodynamic Damping Identification Rigs for Roll and Pitch in Supersonic Wind Tunnel” (HiSAEROD), granted by the Executive Agency for Higher Education, Research, Development and Innovation Funding (UEFISCDI).

## REFERENCES

[1] I. Bunescu, M.-V. Hothazie, M.-V. Pricop and M. Stoican, Roll Damping Measurement on Basic Finner Using Both Forced and Free Methods, in *AIAA Scitech 2023*, National Harbour, 2023.

[2] J. Nicolaides and R. Bolz, On the Pure Rolling Motion of Winged and/or Finned Missiles in Varying Supersonic Flight, *Journal of the Aeronautical Sciences,* vol. **20**, no. 3, pp. 160-168, 1953.

[3] F. Regan, *Roll Damping Moment Measurement for The Basic Finner At Subsonic and Supersonic Speeds*, NAVORD, Maryland, 1964.

[4] H. Murthy, Subsonic and Transonic Roll Damping Measurement on Basic Finner, *Journal of Spacecraft,* vol. **19**, no. 1, pp. 86-87, 1962.
[5] F. Munteanu, INCAS Trisonic Wind Tunnel, *INCAS Bulletin,* (print) ISSN 2066–8201, (online) ISSN 2247–4528, ISSN–L 2066–8201, vol. **1**, http://dx.doi.org/10.13111/2066-8201.2009.1.1.2, 2009.
[6] C. Schueler, L. Ward and A. Hodapp, *Techniques for Measurement of Dynamic Stability Derivatives in Ground Test Facilities*, AGARD, 1967.
[7] R. R. Rhinehart, *Nonlinear Regression Modeling for Engineering Aplications*, Wiley, 2016.
[8] B. L. Uselton and L. M. Jenke, Experimental Missile Pitch- and Roll-Damping Characteristics at Large Angles of Attack, *Spacecraft,* vol. **14**, no. 4, pp. 241-247, 1977.